production, and the *yusLKJ* operon, whose inferred products are similar to lipid catabolism enzymes (fig. S5 and table S1). Use of *lacZ* fused to *yusLKJ* confirmed that high-level expression of the operon was dependent on the signaling protein and on YvbA (Fig. 4B). Also, artificial induction of YvbA synthesis restored the expression of *yusLKJ* to cells doubly mutant for the *sdp* and *yvbA yvaZ* operons (Fig. 4B). We propose that the signaling protein turns on the synthesis of YvbA, which, in turn, causes an increase in lipid oxidation and ATP production. The proposed increase in energy production could be responsible for delaying sporulation, which is triggered by depletion of energy reserves.

Finally, and coming full circle, we found that artificial induction of YvbA synthesis caused a marked drop in cell viability in a manner that was dependent on the *skf* operon (Fig. 4C). Evidently, synthesis of the YvbA transcription factor causes enhanced sensitivity to the sporulation killing factor. It could do so by stimulating the expression of genes involved in energy production, as metabolically active cells are more sensitive to antibiotics than are quiescent cells (*17*, *18*). Also, *yvbA* was previously identified in a screen for genes that inhibit the expression of the gene for σ^W, a regulatory protein that turns on genes involved in detoxification and resistance to antibiotics (*16*, *19*, *20*). Thus, YvbA-mediated repression of the gene for σ^W could heighten sensitivity to the killing factor by suppressing the antibiosis stress response.

We conclude that sporulating cells of *B. subtilis* are cannibalistic, feeding on their siblings in order to delay committing to spore formation. Because sporulation becomes irreversible after its earliest stage, delaying spore formation as long as possible might be beneficial, as a cell that is committed to spore formation could be at a disadvantage relative to other cells should nutrient deprivation prove to be fleeting. Wild (but not laboratory) strains have been found to assemble into multicellular structures in which spore formation preferentially takes place at the apical tips (*21*). Perhaps the killing factor and signaling protein influence the timing and localization of spore formation in these fruiting-body-like structures. Fruiting body formation by the unrelated spore-forming bacterium *Myxococcus xanthus* is reported to involve lysis of nonsporulating cells (*22*). Conceivably, this killing is mediated by cells in the developing fruiting body that have entered the pathway to sporulate. It will be interesting to see whether the killing of genetically identical siblings is a widespread feature of the dynamics of bacterial populations.

References and Notes

1. P. J. Piggot, J. G. Coote, *Bacteriol. Rev.* **40,** 908 (1976).
2. P. J. Piggot, R. Losick, in Bacillus subtilis *and Its Closest Relatives: From Genes to Cells*, A. L. Sonenshein, J. A. Hoch, R. Losick, Eds. (ASM Press, Washington, DC, 2002), pp. 473–481.
3. A. L. Sonenshein, in *Prokaryotic Development*, Y. V. Brun, L. J. Shimkets, Eds. (ASM Press, Washington, DC, 2000), pp. 133–150.
4. A. L. Sonenshein, in *Bacterial Stress Responses*, G. Storz , R. Hengge-Aronis, Eds. (ASM Press, Washington, DC, 2000), pp. 199–215.
5. D. Burbulys, K. A. Trach, J. A. Hoch, *Cell* **64,** 545 (1991).
6. P. Fawcett, P. Eichenberger, R. Losick, P. Youngman, *Proc. Natl. Acad. Sci. U.S.A.* **97,** 8063 (2000).
7. R. Kolter, F. Moreno, *Annu. Rev. Microbiol.* **46**, 141 (1992).
8. R. J. Siezen, O. P. Kuipers, W. M. de Vos, *Antonie Van Leeuwenhoek* **69,** 171 (1996).
9. D. Lin, L.-J. Qu, H. Gu, Z. Chen, *J. Appl. Microbiol.* **91,** 1044 (2001).
10. G. Zheng, L. Z. Yan, J. C. Vederas, P. Zuber, *J. Bacteriol.* **181,** 7346 (1999).
11. J. Pei, N. V. Grishin, *Trends Biochem. Sci.* **26**, 275 (2001).
12. Single-letter abbreviations for the amino acid residues are as follows: A, Ala; C, Cys; D, Asp; E, Glu; F, Phe; G, Gly; H, His; I, Ile; K, Lys; L, Leu; M, Met; N, Asn; P, Pro; Q, Gln; R, Arg; S, Ser; T, Thr; V, Val; W, Trp; X, any amino acid; and Y, Tyr.
13. P. Schaeffer, J. Millet, J. P. Aubert, *Proc. Natl. Acad. Sci. U.S.A.* **54,** 704 (1965).
14. J. D. Chung, G. Stephanopoulos, K. Ireton, A. D. Grossman, *J. Bacteriol.* **176,** 1977 (1994).
15. Of particular interest, accelerated sporulation was observed on solid but not in liquid medium; see supporting text on *Science* Online.
16. J. E. González-Pastor, E. Hobbs, R. Losick, data not shown.
17. M. R. Brown, D. G. Allison, P. Gilbert, *J. Antimicrob. Chemother.* **22,** 777 (1988).
18. R. M. Cozens *et al.*, *Antimicrob. Agents Chemother.* **29,** 797 (1986).
19. M. S. Turner, J. D. Helmann, *J. Bacteriol.* **182,** 5202 (2000).
20. M. Cao, T. Wang, R. Ye, J. D. Helmann, *Mol. Microbiol.* **45**, 1267 (2002).
21. S. S. Branda, J. E. Gonzalez-Pastor, S. Ben-Yehuda, R. Losick, R. Kolter, *Proc. Natl. Acad. Sci. U.S.A.* **98**, 11621 (2001).
22. J. W. Wireman, M. Dworkin, *Science* **189**, 516 (1975).
23. F. Kunst *et al.*, *Nature* **390**, 249 (1997).

24. We are grateful to S. Ben-Yehuda for the *sdpC* mutant and contributing to its characterization; P. Eichenberger and J. M. Ranz for help with the DNA microarray experiments; W. Lane for Edman sequencing; and A. L. Sonenshein, P. Piggot, D. Hartl, D. Haig, A. Murray, M. Fujita and members of the Losick laboratory for helpful advice. This work was supported by NIH grant (GM18568) to R.L. J.E.G.-P. was supported by a Ministerio de Educación y Ciencia Postdoctoral Fellowship (Spain). E.C.H. was supported by an NSF Graduate Research Fellowship.

Supporting Online Material

www.sciencemag.org/cgi/content/full/1086462/DC1
Material and Methods
SOM Text
Figs. S1 to S5
Tables S1 and S2
References

5 May 2003; accepted 6 June 2003
Published online 19 June 2003;
10.1126/science.1086462
Include this information when citing this paper.

VDAC2 Inhibits BAK Activation and Mitochondrial Apoptosis

Emily H.-Y. Cheng,[1] Tatiana V. Sheiko,[2] Jill K. Fisher,[1] William J. Craigen,[2] Stanley J. Korsmeyer[1]*

The multidomain proapoptotic molecules BAK or BAX are required to initiate the mitochondrial pathway of apoptosis. How cells maintain the potentially lethal proapoptotic effector BAK in a monomeric inactive conformation at mitochondria is unknown. In viable cells, we found BAK complexed with mitochondrial outer-membrane protein VDAC2, a VDAC isoform present in low abundance that interacts specifically with the inactive conformer of BAK. Cells deficient in VDAC2, but not cells lacking the more abundant VDAC1, exhibited enhanced BAK oligomerization and were more susceptible to apoptotic death. Conversely, overexpression of VDAC2 selectively prevented BAK activation and inhibited the mitochondrial apoptotic pathway. Death signals activate "BH3-only" molecules such as tBID, BIM, or BAD, which displace VDAC2 from BAK, enabling homo-oligomerization of BAK and apoptosis. Thus, VDAC2, an isoform restricted to mammals, regulates the activity of BAK and provides a connection between mitochondrial physiology and the core apoptotic pathway.

The BCL-2 family of pro- and antiapoptotic proteins constitutes a critical control point for apoptosis (*1*, *2*). A combination of genetic and biochemical approaches has helped to order the components of the mammalian cell death pathway. The upstream "BH3-only" family members respond to select death signals and subsequently trigger the activation of the multidomain death effectors BAX and BAK (*3*–*5*). BAX and BAK constitute an essential gateway to the intrinsic death pathway operating at the level of both mitochondria and endoplasmic reticulum (ER) Ca^{2+} dynamics (*3*, *6*). Activated homo-oligomerized BAX or BAK results in the permeabilization of the mitochondrial outer membrane (MOM) and the

[1]Howard Hughes Medical Institute, Dana-Farber Cancer Institute, Harvard Medical School, Boston, MA 02115, USA. [2]Department of Molecular and Human Genetics, Baylor College of Medicine, Houston, TX 77030–3498, USA.

*To whom correspondence should be addressed. E-mail: stanley_korsmeyer@dfci.harvard.edu

release of proteins including cytochrome c, which initiates a caspase cascade and contributes to organelle dysfunction (*7*–*9*). Conversely, cells protected by adequate levels of antiapoptotic BCL-2 or BCL-X_L bind and sequester translocated BH3-only molecules in stable complexes, preventing the activation of BAX and BAK (*4*). However, the mechanisms by which viable cells keep the potentially lethal proapoptotic BAX and BAK molecules in check are incompletely understood. Before being exposed to death stimuli, BAX and antiapoptotic BCL-2 members are predominantly in separate subcellular compartments, although upon its activation a portion of BAX can be found in association with BCL-2 (*10*, *11*). A three-dimensional structure of monomeric BAX revealed that its C-terminal α helix occupied its own binding pocket formed by its BH1, BH2, and BH3 domains, which provides one explanation for its inactive status in the cytosol or when loosely attached to membranes (*12*). In contrast, BAK is an integral mitochondrial membrane protein in cells not exposed to death stimuli, and consequently its C-terminal transmembrane domain would not be available to occupy its pocket (*7*, *13*). In viable cells, antiapoptotic BCL-2 family members do not interact appreciably with BAK, although they can interact when BAK is activated by BH3-only family members (fig. S1). Consequently, we investigated whether BAK might be complexed with another resident mitochondrial protein that would regulate its activity.

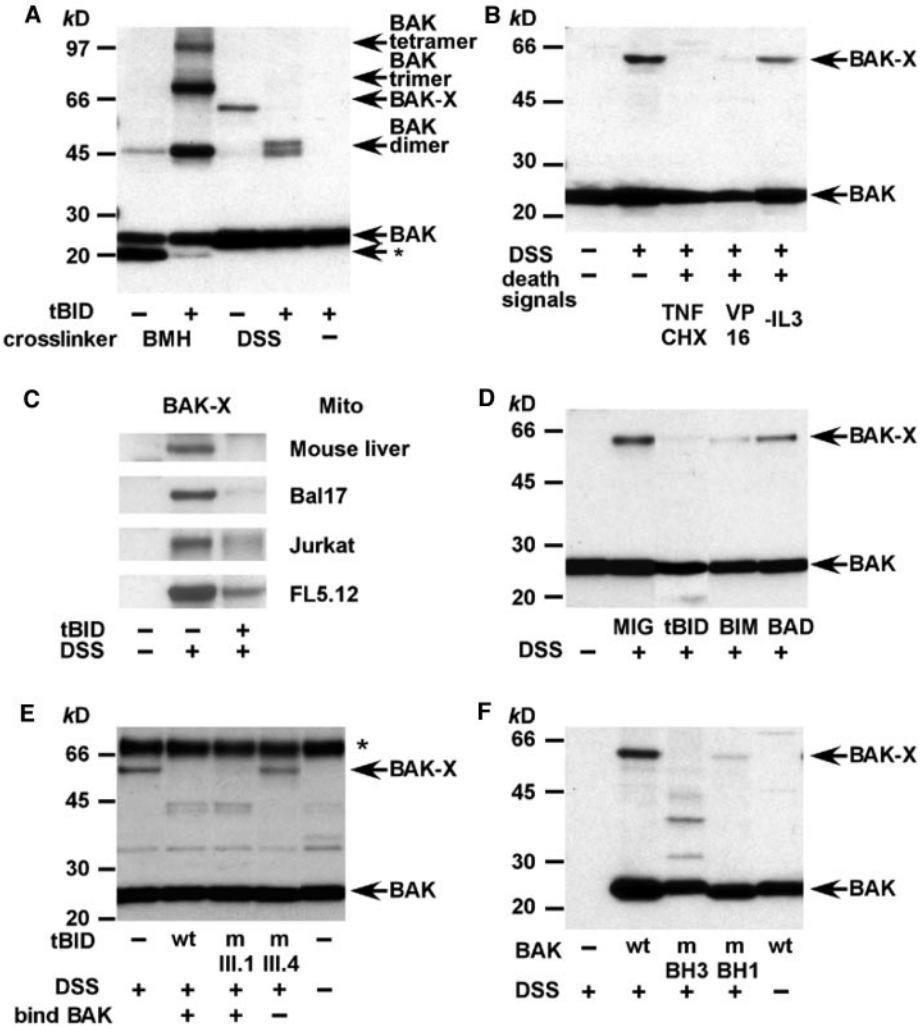

Fig. 1. Characterization of protein X that interacts with BAK. (**A**) Mitochondria (50 μg) isolated from wild-type (wt) MEFs were incubated with recombinant tBID protein (50 ng) at 30°C for 30 min, followed by treatment with the cross-linkers DSS (10 mM) or BMH (10 mM) at room temperature for 30 min. Higher order BAK complexes were identified by an immunoblot developed with an antibody to BAK (anti-BAK). The asterisk denotes an intrachain cross-link of the inactive BAK conformer. (**B**) FL5.12 cells were treated with TNFα plus cyclohexamide (CHX) for 5 hours (lane 3), or etoposide for 24 hours (lane 4), or were deprived of IL-3 for 18 hours (lane 5), followed by incubation with 10 mM DSS. The BAK-X complex was detected in whole-cell lysates by an immunoblot developed with anti-BAK. (**C**) Mitochondria (50 μg) isolated from mouse liver, Bal17, Jurkat, and FL5.12 cells were treated with tBID protein (50 ng) at 30°C for 30 min, followed by DSS cross-linking. The BAK-X complex was detected by an immunoblot developed with anti-BAK. (**D**) Mitochondria isolated from wt MEFs 24 hours after retroviral transduction of tBID, BIM, or BAD were treated with DSS. The BAK-X complex was detected by an immunoblot developed with anti-BAK. (**E**) Isolated liver mitochondria (50 μg) were incubated with 5 μl of in vitro transcribed-translated wt or mutant tBID at 30°C for 30 min, followed by DSS cross-linking. The BAK-X complex was detected by an immunoblot developed with anti-BAK. The asterisk denotes a cross-reactive protein. (**F**) *Bax*, *Bak* doubly deficient MEFs reconstituted with wt or mutant *Bak* (mBH3 or mBH1) were treated with DSS. The BAK-X complex was detected in whole-cell lysates by an immunoblot developed with anti-BAK.

We used protein cross-linkers to search for a candidate protein that interacts with BAK at the mitochondria in viable cells. A mobility-shifted complex of ~60 kD, immunoreactive with an antibody to BAK, was detected after treatment of purified mitochondria (Fig. 1A) or viable whole cells (Fig. 1B) with the cross-linker disuccinimidyl suberate (DSS). We designated as BAK-X this presumed complex between BAK and a candidate interacting protein of ~35 kD. The ~60-kD BAK-X complex was distinct in size compared with BAK homo-oligomers detected by bismaleimidohexane (BMH) cross-linking (Fig. 1A). The same-sized BAK complex was detected in multiple cell lines and in normal liver cells before exposure to death stimuli (Fig. 1C). The BAK-X complex was lost when mitochondria were treated with tBID (Fig. 1, A and C) or cells were treated with death stimuli, including tumor necrosis factor–α (TNF-α), etoposide, or withdrawal of survival factor (Fig. 1B). Expression of BH3-only members BAD, BIM, or tBID killed cells and diminished the amount of BAK-X complex in the cells (Fig. 1D). Studies of mutant tBID molecules indicated that only BH3 domains (BH3 mutation mIII.1, not mIII.4) capable of binding BAK and initiating release of cytochrome c caused dissociation of the BAK-X complex (Fig. 1E) (*7*). In cells expressing BAK mutated within the BH3 domain (L75E), the BAK-X complex was not detected, and in cells expressing a mutated BH1 domain (W122A, G123E, and R124A) the complex was substantially reduced (Fig. 1F). This suggests that X interacts with the BAK pocket formed by the BH1, BH2, and BH3 domains and can be displaced, directly or indirectly, by BH3-only molecules.

To isolate the candidate protein, we expressed N-terminal Flag-tagged BAK in a cell line to facilitate affinity purification. Serial steps of Q Sepharose, hydroxyapatite, MonoQ, and anti-Flag affinity column

chromatography (Fig. 2A) enriched the BAK-X complex from mitochondria (Fig. 2B). Liquid chromatography and tandem mass spectrometry analysis of the complex revealed the presence of two definitive tryptic fragments of the voltage-dependent anion channel 2 (VDAC2) (Fig. 2B). When *vdac2*-deficient embryonic stem (ES) cells were subjected to DSS cross-linking (*14*), no 60-kD BAK-containing complex was detected (Fig. 2C), further implicating VDAC2, but not VDAC1 or VDAC3, as the BAK-interacting protein. Re-expressing VDAC2 in *vdac2*$^{-/-}$ ES cells by retroviral transduction restored the 60-kD complex. The BAK complex was present in cells deficient for the closely related homolog VDAC1 (Fig. 2C). The active conformation of BAK displays more proteolytic susceptibility than the inactive conformer (Fig. 2D). We therefore assessed the pattern of trypsin-digested BAK from isolated mitochondria of wild-type, *vdac2*-deficient, or *vdac1*-deficient cells. The absence of VDAC2 increased the susceptibility of BAK to proteolysis (Fig. 2D). Even before tBID exposure, a substantial portion of BAK in *vdac2*-deficient mitochondria demonstrated a pattern resembling activation (Fig. 2D). These data support a model in which VDAC2, but not VDAC1, regulates the conformation of BAK.

Endogenous BAK, but not BAX, was efficiently coprecipitated with hemagglutinin (HA)–tagged VDAC2 (Fig. 2E). This interaction was noted after solubilization of cell extracts with the zwitterionic detergent CHAPS, which unlike nonionic detergents does not induce a conformational change in BAX or BAK (*15*, *16*). Solubilization of proteins in nonionic NP40 reduced the amount of BAK complexed with VDAC2, also consistent with VDAC2 preferentially interacting with inactive BAK. HA-tagged BAK, but not HA-tagged BAX, coprecipitated endogenous VDAC2 (Fig. 2E). No BCL-2 or BCL-X_L coprecipitated with HA-BAX or HA-BAK in 1% CHAPS (*17*), consistent with VDAC2, but not BCL-2 or BCL-X_L, binding to the inactive conformer of BAK.

Cells doubly deficient for BAX and BAK are resistant to intrinsic death stimuli, whereas cells singly deficient for BAX or BAK are still susceptible (*3*). Because VDAC2 interacts with BAK but not with BAX, we investigated whether VDAC2 could modulate apoptosis mediated by BAK or BAX. VDAC2 might function as an inhibitor of BAK, or VDAC2 itself might function as a proapoptotic factor once released from BAK. To examine these alternatives, we expressed VDAC1 or VDAC2 in *Bax*$^{-/-}$ or *Bak*$^{-/-}$ singly deficient mouse embryonic fibroblasts (MEFs) followed by treatment with staurosporine (STS) or etoposide. Expression of VDAC2 significantly inhibited apoptosis in *Bax*$^{-/-}$ cells that have BAK, but had no effect in *Bak*$^{-/-}$ cells. In contrast, expression of VDAC1 displayed no substantial effect on cell viability (Fig. 3A; fig. S2). tBID, an activated BH3-only molecule, activates BAX and BAK and requires one or the other to induce apoptosis (*3*). Expression of VDAC2 inhibited tBID-induced apoptosis of *Bax*$^{-/-}$ cells but not *Bak*$^{-/-}$ cells, further supporting a selective role for VDAC2 in negatively regulating BAK-dependent apoptosis (Fig. 3B). ES cells deficient for VDAC2, but not those deficient for VDAC1, proved more sensitive to various death stimuli, including STS and etoposide (Fig. 3C). To consolidate these findings, we established *vdac2*$^{-/-}$ MEFs selected from chimeric embryos generated by microinjection of *vdac2*$^{-/-}$ ES cells into wild-type blastocysts. *vdac2*$^{-/-}$ primary MEFs displayed significantly more spontaneous ap-

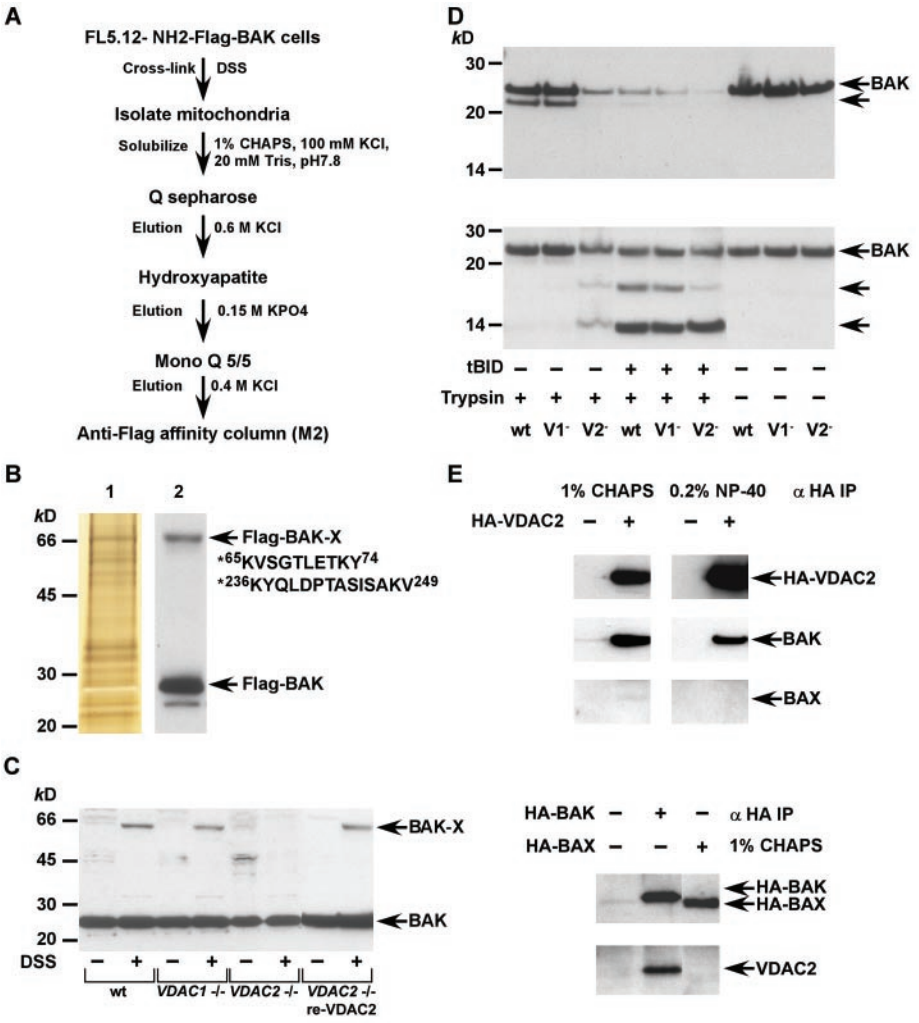

Fig. 2. Identification of VDAC2 as the BAK-interacting partner that regulates BAK conformation. (**A**) Purification scheme for Flag-tagged BAK-X complex. (**B**) Samples of the Flag-peptide eluent from anti-Flag column were analyzed by silver stain (lane 1) and immunoblot developed with anti-BAK (lane 2). The silver-stained band corresponding to Flag-BAK-X was subjected to tryptic digestion and liquid chromatography–tandem mass spectrometry. Asterisks indicate the peptide sequences of VDAC2 revealed by mass spectrometry. (**C**) Cellular extracts (20 μg protein) from wt, *vdac1*$^{-/-}$, *vdac2*$^{-/-}$, or *vdac2*-reconstituted *vdac2*$^{-/-}$ ES cells treated with 10 mM DSS were analyzed by an immunoblot developed with an anti-BAK. Reconstitution of *vdac2* into *vdac2*$^{-/-}$ cells was accomplished by retroviral transduction. (**D**) Mitochondria (50 μg) isolated from wt, *vdac1*$^{-/-}$ (v1^{-}), or *vdac2*$^{-/-}$ (v2^{-}) ES cells were treated with trypsin (30 μg/ml). The trypsin sensitivity pattern of BAK was assessed by immunoblot with two distinct epitope-specific antibodies to BAK (upper panel, anti-BAK NT; lower panel, anti-BAK G23). (**E**) Mitochondria isolated from wt MEFs (upper panel) or *Bax*, *Bak* doubly deficient MEFs (lower panel) transduced with retrovirus expressing N-terminal HA-tagged VDAC2, BAK, or BAX were solubilized in either 1% CHAPS or 0.2% NP-40 buffer, followed by immunoprecipitation with anti-HA. The immunoprecipitates were analyzed by an immunoblot developed with anti-HA–Biotin, anti-BAK, anti-BAX, or anti-VDAC2, as indicated.

optosis during culture ($P \leq 0.0026$) (Fig. 3D; fig. S3, B and C). Moreover, they proved more sensitive to STS and etoposide (Fig. 3D; fig. S3A). Consistent with this result, *vdac2*-null cells were also more sensitive to tunicamycin, which mimics unfolded protein responses thought to reflect ER stress and predominantly uses mitochondrial BAX, BAK (fig. S3B) (*6*). In contrast, *vdac1*$^{-/-}$ or *vdac3*$^{-/-}$ cells were similar in sensitivity to wild-type cells (fig. S3E). Re-expression of VDAC2 to normal physiological levels in *vdac2*$^{-/-}$ MEFs reversed the increased susceptibility to apoptosis (Fig. 3E).

vdac2$^{-/-}$ MEF cells responded to STS with accelerated surface exposure of phosphatidylserine (Fig. 4A), and more *vdac2*$^{-/-}$ cells than wild-type cells lost mitochondrial transmembrane potential as measured by tetramethylrhodamine ethyl ester (TMRE) fluorescence intensity (Fig. 4B). *vdac2*$^{-/-}$ cells treated with STS exhibited partial release of cytochrome c into the cytosol by 3 hours and complete release by 5 hours, times at which wild-type cells had not initiated any release of cytochrome c (Fig. 4C). Immunohistochemistry on wild-type cells confirmed that cytochrome c remained in a punctate mitochondrial pattern at 4 hours after STS treatment but was diffusely cytosolic in *vdac2*-deficient cells (Fig. 4D). *vdac2*$^{-/-}$ cells demonstrated activity of effector caspases 3 and 7 earlier than did wild-type cells after STS treatment (Fig. 4E; fig. S4). In contrast, the responses of wild-type and *vdac2*-deficient cells were similar when the extrinsic death pathway was activated by TNF-α (Fig. 4E). These findings prompted us to examine *vdac2*-null cells for changes occurring before mitochondrial damage. BAK had undergone oligomerization within 5 hours after STS treatment in *vdac2*$^{-/-}$ cells but not in wild-type cells, as assessed by gel filtration (Fig. 4F) (*16*). This conformational activation of BAK coincides with the timing of complete release of cytochrome c and peak caspase activity. In contrast, wild-type cells did not display BAK oligomerization until ~10 hours after treatment (*17*). In the absence of VDAC2, the cross-linker BMH did not efficiently capture these higher order BAK multimers, suggesting that their conformation was altered (*17*). We conclude that in the absence of inhibition by VDAC2, BAK demonstrates an enhanced allosteric conformational activation resulting in the release of cytochrome c, caspase activation, and mitochondrial dysfunction responsible for an increased susceptibility to apoptotic death. Of note, in the absence of VDAC2, only a portion of BAK undergoes a spontaneous conformational change; full activation requires a death stimulus such as tBID or STS (Figs. 2D and 4F).

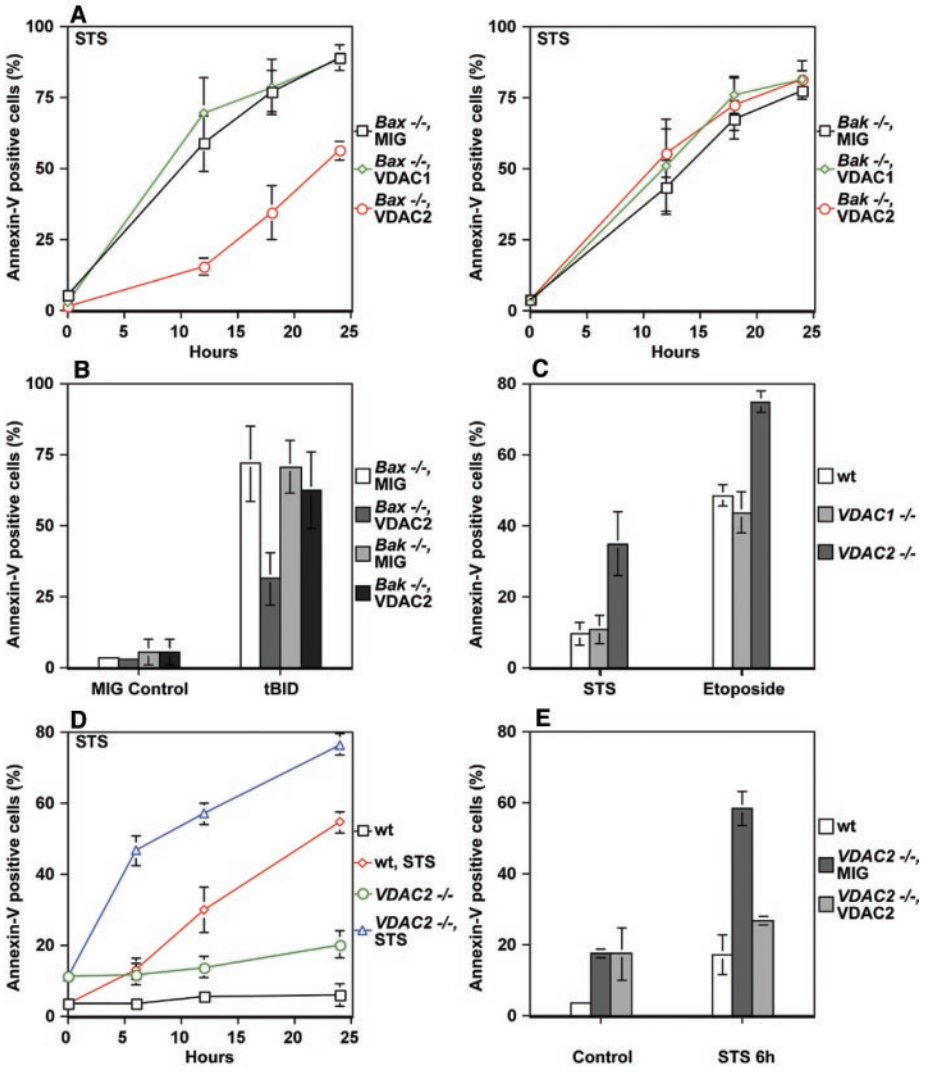

Fig. 3. Regulation of BAK-dependent apoptosis by VDAC2. Values shown are mean ± 1 SD of three independent experiments. (**A**) *Bax*$^{-/-}$ or *Bak*$^{-/-}$ MEFs, 2 days after retroviral expression of VDAC1, VDAC2, or green fluorescent protein (GFP) (MIG vector control), were treated with 1.2 μM STS. Cell death was quantitated by flow cytometric detection of Annexin-V staining at the indicated time points. (**B**) *Bax*$^{-/-}$ or *Bak*$^{-/-}$ MEFs, 2 days after retroviral expression of VDAC2 or GFP (MIG vector control), were infected with tBID-expressing retrovirus. Cell death was quantitated by flow cytometric detection of Annexin-V staining at 24 hours. (**C**) Wt, *vdac1*$^{-/-}$, or *vdac2*$^{-/-}$ ES cells were treated with STS (1.2 μM) for 6 hours or etoposide (10 μg/ml) for 12 hours. Cell death was quantitated by flow cytometric detection of Annexin-V staining. (**D**) Primary wt or *vdac2*$^{-/-}$ MEFs were treated with STS (1.2 μM). Cell death was quantitated by flow cytometric detection of Annexin-V staining at indicated time points. (Spontaneous death at 24 hours culture for wt 5.5 ± 2.3% and vdac2-null MEFs 20.1 ± 3.9%; $P \leq .0026$). (**E**) Primary *vdac2*$^{-/-}$ MEFs were infected with retrovirus expressing GFP (MIG vector control) or VDAC2-IRES (internal ribosomal entry site)–GFP. At 36 hours, the GFP-positive cells isolated by MoFlo (DakoCytomation, Carpinteria, CA) sorting were treated with 1.2 μM STS for 6 hours. Cell death was quantitated by flow cytometric detection of Annexin-V staining.

VDAC proteins constitute the major pathway for metabolic exchange across the MOM, yet the existence of three mammalian isoforms (VDAC1, VDAC2, and VDAC3) suggests that they may each have some distinct physiological role (*14*, *18*, *19*). VDAC has been proposed in several contexts as a participant in cell death. VDAC is a candidate component of the permeability transition pore, thought to participate in both apoptotic and necrotic cell deaths (*20*, *21*). However, reports of functional interactions between cell death regulators and VDAC, specifically the highly abundant VDAC1 isoform, vary markedly. Antiapoptotic BCL-X_L reportedly closes VDAC to prevent cytochrome c release, whereas proapoptotic BAX may promote VDAC opening or form a VDAC-BAX hybrid channel that releases cytochrome c (*22*, *23*). Other evidence indicates that BCL-X_L promotes an open configura-

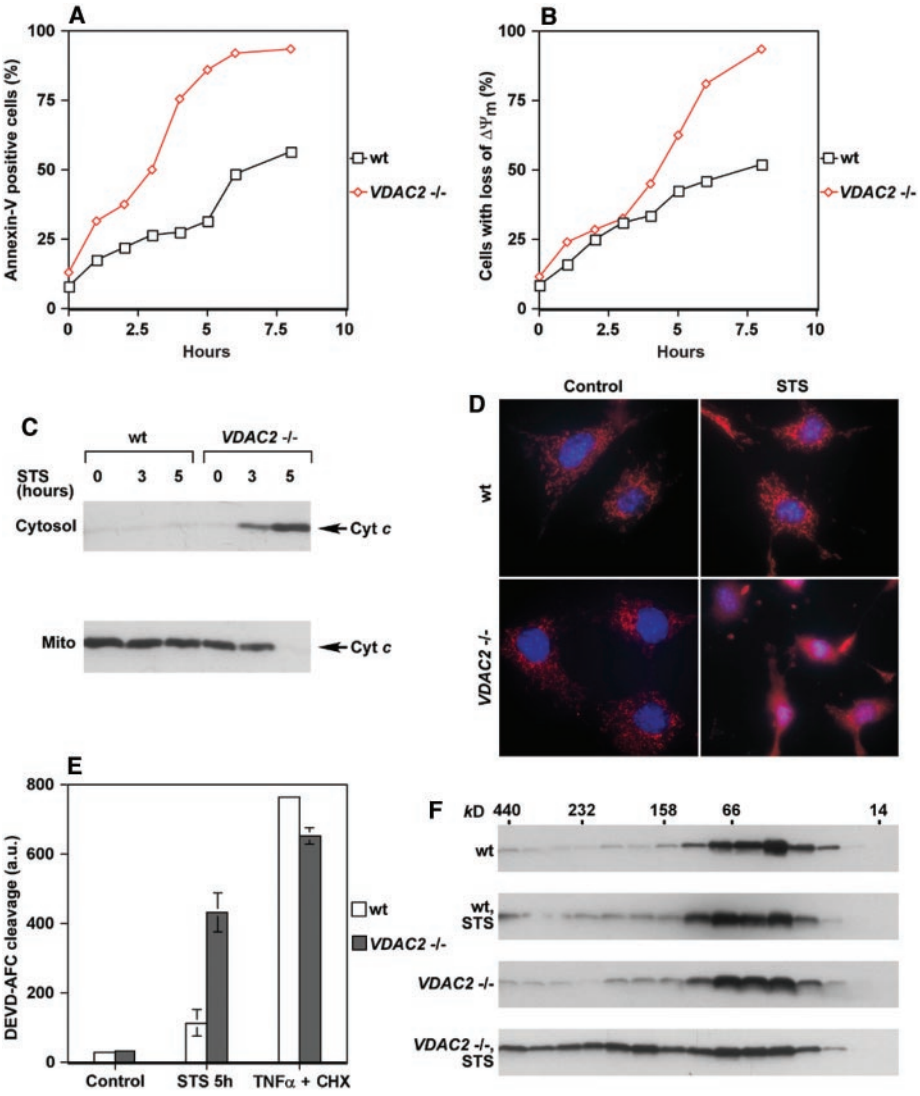

Fig. 4. Comparison of apoptotic hallmarks in *vdac2*$^{-/-}$ and wt cells. (**A**) SV40-transformed wt or *vdac2*$^{-/-}$ MEFs were treated with 1 μM STS and cell death was quantitated by flow cytometric detection of Annexin-V staining at indicated time points. Values shown are the means of two independent experiments. The same increased susceptibility to apoptosis was noted in the *vdac2*-null cell line as in primary MEFs. (**B**) The mitochondrial membrane potential ($\Delta\psi_m$) of wt or *vdac2*$^{-/-}$ MEF cell lines, after treatment with 1 μM STS, was assessed by flow cytometric detection of TMRE uptake at indicated time points. Values shown are means of two independent experiments. (**C**) Wt or *vdac2*$^{-/-}$ MEF cell lines treated with STS (1 μM) were subcellularly fractionated (*30*) at indicated time points. Cytochrome c distribution in the cytosol versus mitochondria was assessed by immunoblot developed with an antibody to cytochrome c. (**D**) Two-color fluorescence microscopy of wt and *vdac2*$^{-/-}$ MEF lines at 4 hours after 1 μM STS. Red indicates cytochrome c and blue is Hoechst staining of DNA. Analysis of multiple fields indicates that 83% of *vdac2*$^{-/-}$ cells, but only 16% of wt cells, display diffuse cytosolic staining for cytochrome c at 4 hours post-STS. (**E**) Cell lysates from wt or *vdac2*$^{-/-}$ MEF lines treated with 1 μM STS for 5 hours or with TNF-α (2 ng/ml) plus cyclohexamide (2 μg/ml) for 12 hours were assessed for effector caspase activity by a DEVD-AFC cleavage assay. Values shown are the mean ± 1 SD of three independent experiments. (**F**) Mitochondria isolated from wt or *vdac2*$^{-/-}$ MEF cell lines with or without treatment with STS for 5 hours were solubilized in stringent conditions of 2% CHAPS buffer and 300 mM NaCl capable of detecting the shift of BAK from a low molecular weight inactive form to a higher order homo-oligomeric complex (*16*). Protein lysate (200 μg) was subjected to Superdex 200 (HR 10/30) gel filtration column chromatography. Fractions were analyzed by an immunoblot developed with anti-BAK. Under milder conditions of 1% CHAPS and 150 mM NaCl, a portion of BAK coelutes with VDAC2 in mitochondrial lysates from wt cells before exposure to a death stimulus, consistent with their copresence in a complex (not shown).

tion of VDAC to maintain adenosine diphosphate–adenosine triphosphate exchange and cell viability (*24*, *25*). Whereas *vdac3*-deficient mice are viable, *vdac1*-deficient mice exhibit a partial, strain-specific embryonic lethality, and *vdac2*-deficient embryos are nonviable (*26*–*29*). Here we define a distinctive physiological role in vivo for the VDAC2 isoform as a specific inhibitor of BAK-dependent mitochondrial apoptosis. BAK but not BAX interacts with VDAC2, an isoform restricted to mammals, but not with the more abundant VDAC1. This suggests that, as BCL-2 proapoptotic effectors expanded in number and complexity, a physiological component of the mitochondrial membrane, VDAC2, coevolved to regulate cell death. This physical interaction provides an opportunity for communication between mitochondrial metabolism and apoptosis.

References and Notes

1. S. Cory, J. M. Adams, *Nature Rev. Cancer* **2**, 647 (2002).
2. D. R. Green, J. C. Reed, *Science* **281**, 1309 (1998).
3. M. C. Wei *et al.*, *Science* **292**, 727 (2001).
4. E. H. Cheng *et al.*, *Mol. Cell* **8**, 705 (2001).
5. W. X. Zong, T. Lindsten, A. J. Ross, G. R. MacGregor, C. B. Thompson, *Genes Dev.* **15**, 1481 (2001).
6. L. Scorrano *et al.*, *Science* **300**, 135 (2003).
7. M. C. Wei *et al.*, *Genes Dev.* **14**, 2060 (2000).
8. S. Desagher *et al.*, *J. Cell Biol.* **144**, 891 (1999).
9. P. Li *et al.*, *Cell* **91**, 479 (1997).
10. Y. T. Hsu, K. G. Wolter, R. J. Youle, *Proc. Natl. Acad. Sci. U.S.A.* **94**, 3668 (1997).
11. A. Gross, J. Jockel, M. C. Wei, S. J. Korsmeyer, *EMBO J.* **17**, 3878 (1998).
12. M. Suzuki, R. J. Youle, N. Tjandra, *Cell* **103**, 645 (2000).
13. G. J. Griffiths *et al.*, *J. Cell Biol.* **144**, 903 (1999).
14. S. Wu, M. J. Sampson, W. K. Decker, W. J. Craigen, *Biochim. Biophys. Acta* **1452**, 68 (1999).
15. Y. T. Hsu, R. J. Youle, *J. Biol. Chem.* **273**, 10777 (1998).
16. X. Roucou, S. Montessuit, B. Antonsson, J. C. Martinou, *Biochem. J.* **368**, 915 (2002).
17. E.-H. Cheng, S. J. Korsmeyer, unpublished data.
18. M. J. Sampson, R. S. Lovell, W. J. Craigen, *J. Biol. Chem.* **272**, 18966 (1997).
19. X. Xu, W. Decker, M. J. Sampson, W. J. Craigen, M. Colombini, *J. Membr. Biol.* **170**, 89 (1999).
20. P. Bernardi, *Physiol. Rev.* **79**, 1127 (1999).
21. N. Zamzami, G. Kroemer, *Nature Rev. Mol. Cell Biol.* **2**, 67 (2001).
22. S. Shimizu, M. Narita, Y. Tsujimoto, *Nature* **399**, 483 (1999).
23. S. Shimizu, T. Ide, T. Yanagida, Y. Tsujimoto, *J. Biol. Chem.* **275**, 12321 (2000).
24. M. G. Vander Heiden, N. S. Chandel, P. T. Schumacker, C. B. Thompson, *Mol. Cell* **3**, 159 (1999).
25. M. G. Vander Heiden *et al.*, *J. Biol. Chem.* **276**, 19414 (2001).
26. K. Anflous, D. D. Armstrong, W. J. Craigen, *J. Biol. Chem.* **276**, 1954 (2001).
27. M. J. Sampson *et al.*, *J. Biol. Chem.* **276**, 39206 (2001).
28. E. J. Weeber *et al.*, *J. Biol. Chem.* **277**, 18891 (2002).
29. W. J. Craigen, T. V. Sheiko, unpublished data.
30. Materials and methods are available as supporting material on *Science* Online.

31. We thank J. J.-D. Hsieh for helpful discussions and E. Smith for editorial assistance. W.J.C. is supported by NIH grant NS42319. This work is supported in part by NIH grant R37CA50239. E.M.-Y.C. is supported by a Beckenstein Fellowship.

Supporting Online Material

www.sciencemag.org/cgi/content/full/301/5632/513/DC1

Materials and Methods

Figs. S1 to S4

28 February 2003; accepted 17 June 2003